Bandwidth Efficient Cooperative TDOA Computation for Multicarrier Signals of Opportunity

Richard K. Martin, Jamie S. Velotta, and John F. Raquet, *Member, IEEE*

***Abstract*—Source localization, the problem of determining the physical location of an acoustic or wireless emitter, is commonly encountered in sensor networks which are attempting to locate and track an emitter. Similarly, in navigation systems that do not rely on the global positioning system (GPS), "signals of opportunity" (existing wireless infrastructure) can be used as ad hoc navigation beacons, and the goal is to determine their location relative to a receiver and thus deduce the receiver's position. These two research problems have a very similar mathematical structure. Specifically, in either the source localization or navigation problem, one common approach relies on time difference of arrival (TDOA) measurements to multiple sensors. In this paper, we investigate a bandwidth efficient method of TDOA computation when the signals of opportunity use multicarrier modulation. By exploiting the structure of the multicarrier transmission, much less information needs to be exchanged between sensors compared to the standard cross correlation approach. Analytic and simulation results quantify the performance of the proposed algorithm as a function of the signal-to-noise ratio (SNR) and the bandwidth between the sensors.**

***Index Terms*—Multicarrier, navigation, orthogonal frequency division multiplexing, source localization.**

I. Introduction

Accurate position measurement is important for many source localization and navigation problems. Sensor networks are becoming increasingly popular for applications such as determining the position of the source of a wireless transmission [1]. Similarly, microphone arrays can be used to determine the location of an acoustic source [2], to aid automatic camera tracking [3], or determination of the source of sniper fire [4]. This problem is generally referred to as "source localization." The converse, but mathematically similar, problem is navigation via signals of opportunity [5], [6], [7], [8]. In this navigation problem, the premise is to use existing wireless infrastructure, such as radio and television towers at known locations, to determine the position of a mobile receiver. Although the global positioning system (GPS) usually provides worldwide high-accuracy position measurements, it requires lines of sight to multiple satellites; hence, it is ill-suited to use indoors, underground, or in urban canyons. Moreover, in the presence of radio-frequency interference or jamming, GPS may be unavailable. Thus, alternative methods of navigation and positioning are of interest, either as a backup or for use in areas unreachable by satellites.

For both the source localization or the navigation problem, the intent is to determine the relative position of the transmitter and the receiver. Measurements that can be taken to aid this process include the angle of arrival (AOA) [1], the received signal strength (RSS) [2], [9], or the time difference of arrival (TDOA) at multiple receivers [10]. The drawback of AOA measurements is that the quality of the final position estimate degrades rapidly as the receivers move away from the source. RSS is frequently used, but it generally requires assuming that the transmitted power and the path loss exponent are known (or are included as additional parameters to be estimated [11]), that there is no multipath or shadowing, and that the transmitter is isotropic—assumptions which are generally not valid. Thus, in some applications, TDOA is an attractive alternative. Moreover, TDOA can be combined with AOA or RSS measurements to improve the accuracy of the estimator [12], [13].

In this paper, we focus on TDOA-based methods. It is possible to directly determine a position estimate from the received data signals. However, in [14] and [15], it was shown that for TDOA methods, the Cramér–Rao lower bound on the position estimate can be obtained by first estimating the TDOAs and then using the TDOAs to estimate the position. Thus, in this paper, we focus on TDOA estimation, rather than direct position estimation.

In TDOA-based methods, there must be either two transmitters sending the same signal or two spatially separated receivers measuring the same transmission. Usually only one transmitter is available, hence multiple sensors or receivers must cooperate by sharing data. One difficulty that arises from this is that the sharing of data requires significant bandwidth (as opposed to RSS or AOA-based methods). Specifically, TDOA measurements are often determined from the generalized cross correlation of the two received signals [3], [16], which requires that one of the two sensors involved in each TDOA computation retransmit a long portion of the signal it receives to the other sensor involved in the computation. However, this may require a large amount of bandwidth and power, which are limited resources for mobile, wireless devices. Thus, the main goal of this paper is to reduce the amount of data that must be shared between sensors in order to perform TDOA computation. In

Manuscript received October 12, 2007; accepted December 31, 2008. First published February 06, 2009; current version published May 15, 2009. The associate editor coordinating the review of this manuscript and approving it for publication was Dr. Zhi Tian. J. S. Velotta conducted this work while at The Air Force Institute of Technology. This work was funded in part by the Air Force Research Labs, Sensors Directorate; and by the Air Force Office of Scientific Research. The views expressed in this paper are those of the author and do not reflect the official policy or position of the United States Air Force, Department of Defense, or the U.S. Government. This document has been approved for public release; distribution unlimited.

R. K. Martin and J. F. Raquet are with the Department of Electrical and Computer Engineering, The Air Force Institute of Technology (AFIT), Wright-Patterson AFB, OH 45433 USA (e-mail: richard.martin@afit.edu; john.raquet@afit.edu).

J. S. Velotta was with The Air Force Institute of Technology (AFIT), Wright-Patterson AFB, OH 45433 USA. He is now with The Boeing Company, Huntsville, AL 35824 USA (e-mail: jsvelotta@hotmail.com).

Color versions of one or more of the figures in this paper are available online at http://ieeexplore.ieee.org.

Digital Object Identifier 10.1109/TSP.2009.2014813

particular, we show that the structure of multicarrier modulation allows for a partially decentralized form of cross correlation to be performed by retransmitting significantly less data between sensors.

The assumption that the transmitter uses multicarrier modulation, also known as orthogonal-frequency-division multiplexing (OFDM), is not a very onerous restriction, since a large number of emerging systems are multicarrier based. Examples include various wireless personal, local, and metropolitan area networks (PANs/LANs/MANs), digital video and audio broadcasts in Europe (DVB/DAB), the terrestrial repeaters used by both brands of satellite radio in North America, and even some wireline standards such as digital subscriber lines (DSL) and power line communications (PLC).

Multicarrier systems use a more highly structured transmission format than many single carrier schemes. Of particular note, the beginning and end of each block of data are identical, due to the presence of a cyclic prefix inserted before each block. Thus, each sensor can identify block boundaries by looking for this repetition, which does not require knowledge of the transmitted signal (i.e., it is noncooperative, or "blind"). The sensors can independently locate the block boundaries without any cooperation amongst them, and then can each calculate some statistical feature (e.g., the sample mean or variance) of each block. Then one sensor can transmit the sequence of block reception times and the associated feature values to another sensor, rather than retransmitting the entire signal. We will show that for the initial position estimation, this partially decentralized computation of the cross correlation can be used to obtain the same performance as the centralized approach with two to three times less bandwidth; or alternatively, if the bandwidth use is held constant, the proposed approach yields the same performance as the centralized version at 3 to 5 dB lower signal-to-noise ratios (SNRs). Moreover, once the position has been established, tracking the position updates requires several orders less data than the standard cross-correlation approach.

There are several other papers in the literature that perform positioning using multicarrier signals. The main difference between most of this work and our work is that our work does not make use of training data in the transmitter. The work in [17] is somewhat similar to our work insofar as the authors estimate the block boundaries of the multicarrier structure. However, their work is based on the Schmidl–Cox [18] and Minn [19] synchronization algorithms, both of which make use of a specially-designed training signal. Thus, their work is limited to cooperative schemes. Similarly, [20] discussed an indoor positioning system in which all transmitters and receivers are cooperative and specifically designed for positioning accuracy; [21] makes use of a known transmitted signal by looking for time-delay-induced phase rotations across subcarriers at the receiver; and [22] and [23] correlate the received signals with the training sequence used by IEEE 802.11a wireless LANs. If available, training can also be used to reduce errors due to multipath and/or non-line-of-sight (NLOS) errors [24]. However, our proposed method is blind, i.e., we do not assume training is available, which is a critical assumption for military, law enforcement, and other surveillance applications.

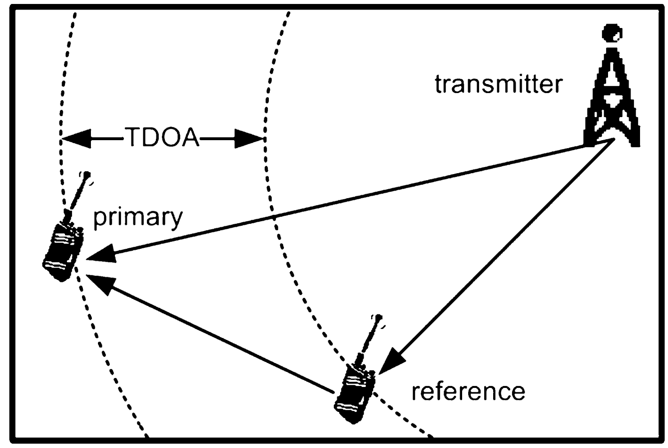

Fig. 1. Geometry of TDOA computation for source localization or navigation.

There are also two other positioning methods which are tangentially relevant, since they involve multicarrier signals. In [25], the authors switch between standard TDOA positioning and Cell ID positioning (simply making use of knowledge of which cell the mobile is in a cellular system). The Cell ID method is used only when received power levels indicate the mobile is near the base station. As such, it could be considered complimentary to our approach, which refines the TDOA method of positioning. In [26], each receiver is assumed to have an antenna array, allowing for extraction of both time of arrival and direction of arrival information, and the data from all antenna elements of all receivers at all times is available in a central location. Moreover, training data is assumed to be available. In contrast, our approach does not make use of antenna arrays, does not use training, and attempts to minimize the amount of bandwidth needed to gather information in a central location.

In Section II, we outline the system model and our assumptions. In Section III, we describe the proposed approach. In Section IV, we discuss computational complexity and other resource considerations. In Section V, the performance of the standard and the proposed approach is presented analytically, as a function of the sensor-to-sensor bandwidth and the SNR; and these results are verified via simulations in Section VI. Section VII concludes the paper.

II. System Model

The geometry of the sensors involved in a single TDOA computation from a single transmitter is depicted in Fig. 1. The transmitter can be either a source to be localized or a signal of opportunity to be used for navigation. The sensor that computes the centralized portion of the cross-correlation is denoted the "primary" sensor. This would be the mobile receiver in a navigation application, and each sensor can take this role in turn in a source localization problem. The sensor which shares information with the primary is denoted the "reference" sensor. In general, additional transmitters and/or reference sensors are required in order to obtain multiple TDOA measurements, but for simplicity we only show one of each. We assume that the transmitter has a line of sight (LOS) to the reference sensor and a LOS to the primary whose location is to be determined. There must be a reliable communication link between the reference

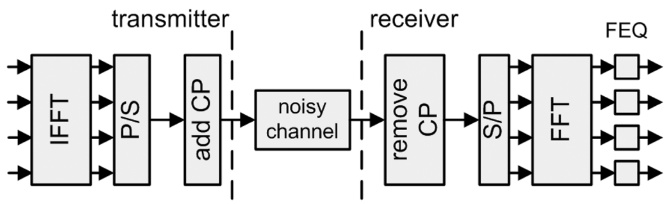

Fig. 2. Block diagram of a multicarrier transmitter and receiver. (I)FFT: (inverse) fast Fourier transform, CP: cyclic prefix, P/S: parallel-to-serial, S/P: serial to parallel, FEQ: frequency-domain equalizer.

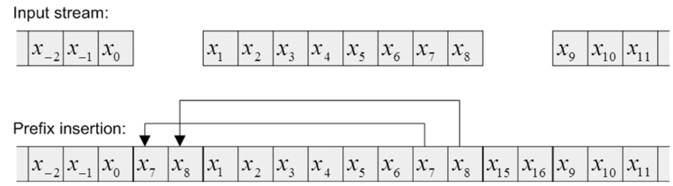

Fig. 3. Insertion of the cyclic prefix, for an FFT size of $N = 8$ and a CP length of $\nu = 2$.

and the primary, but it need not be LOS. The location of the reference is assumed known, and either the position of the transmitter (for navigation) or the primary (for source localization) must be known. The reference gathers information about the received signal and passes a portion of the information on to the primary, and the primary compares its received signal to the data from the reference in order to compute the TDOA. The intent is that the amount of bandwidth that the reference uses to transmit to the primary be as small as possible.

In source localization, there are typically many receivers at known locations and one transmitter at an unknown location. In navigation, there are many transmitters at known locations (with distinct signals) and at least two receivers. Often one of the receiver locations is assumed known, but that is not required if there are enough transmitters. In either problem, the first step is to compute a TDOA from each transmitter to each pair of receivers, which is the problem we focus on. The second step is to use the TDOAs to estimate any unknown positions of transmitters or receivers, as well as any clock offsets. This second step is not our focus, and there are many centralized and decentralized solutions in the literature [27]–[29].

The "full knowledge" approach to TDOA computation would be to have the reference rebroadcast its entire received signal to the primary, and then have the primary cross-correlate the signal from the transmitter and the signal from the reference. However, this is wasteful of bandwidth. A lower complexity approach is to look for notable events that can be separately located in the received signals at the reference and the primary. For example, occasional sharp spikes might occur in the transmitted signal, and both receivers can locate and compare the times when the received signal exceeds some threshold. Then the reference only needs to transmit the times at which the events occurred, and the primary can correlate this with its own record of when the events occurred. The main drawback of this approach is that the events in question may be sensitive to noise, because in a low SNR environment, significant spikes are more likely to be due to the noise than the signal. In addition, some signals do not contain identifiable "features," even in high SNR conditions. In the next section, we will discuss how the block structure of multicarrier modulation naturally lends itself to identification of events of this sort. First, however, we present the mathematical model of multicarrier modulation.

Fig. 2 shows the multicarrier system model. The idea is to break up a frequency-selective multipath channel into a bank of flat narrowband channels. This can be accomplished by parsing the source data into N parallel lower rate data streams, and modulating them with linearly spaced carrier frequencies. Equivalently, we can apply an inverse fast Fourier transform (FFT) to each successive block of N data samples. Then equalization can be done after a demodulating FFT at the receiver, simply by inverting the channel in the frequency domain.

This method of equalization is enabled by the fact that circular convolution in time is equivalent to elementwise multiplication in frequency. Since the channel induces a *linear* convolution with the data, the convolution is made circular inserting a cyclic prefix (CP) of length ν at the start of each block, as shown in Fig. 3. The CP is a copy of the last ν samples of each block, and it extends each block from N to $M = N + \nu$ samples. Although the purpose of the CP is multipath mitigation, we will make use of it to ease the TDOA computation in the next section.

The notation is as follows. The discrete-time transmitted data stream will be denoted $x(i)$. The redundancy induced by the CP causes the source data to obey

$$x\left(Mk+i\right) = x\left(Mk+i+N\right), \quad i \in \{1, \ldots, \nu\}, \quad -\infty < k < \infty \tag{1}$$

where k denotes the block index and i is the sample index within the block. We assume that the inverse fast Fourier transform (IFFT) input is uncorrelated, and by the central limit theorem the IFFT output x is approximately Gaussian. Also, x is uncorrelated with itself aside from the repetition indicated by (1). We do not explicitly deal with oversampling, but it could be included to improve the resolution of the TDOA estimate; thus, the sample period T_s is a fraction $1/M$ of the OFDM block duration. The sampled received signals at the reference and the primary are

$$\begin{aligned} y_{\mathrm{ref}}(i) &= \sum_j h_{\mathrm{ref}}(j)x(i-j) + n_{\mathrm{ref}}(i) \\ y_{\mathrm{pri}}(i) &= \sum_j h_{\mathrm{pri}}(j)x(i-j) + n_{\mathrm{pri}}(i). \end{aligned} \tag{2}$$

Here, h_{ref} and h_{pri} are multipath channels consisting of Ricean fading LOS paths at delays $j = \delta_{\mathrm{ref}}$ and $j = \delta_{\mathrm{pri}}$ (in samples) respectively, as well as other Rayleigh fading paths at longer delays. Our simulations use up to four total rays of multipath. As in most TDOA positioning literature, we assume that the LOS path dominates the multipath [14], [15], [26]. Specifically, we assume that the sum of the coefficient variances is on the order of or less than the mean squared of the LOS path. If this is not true, then any blind method of TDOA computation will have significant difficulty. Additive noise is represented by $n_{\mathrm{ref}}(i)$ and $n_{\mathrm{pri}}(i)$. The signal and noise powers are $\sigma_x^2, \sigma_{\mathrm{ref}}^2$, and σ_{pri}^2. The TDOA can be written as

$$T = (\delta_{\mathrm{pri}} - \delta_{\mathrm{ref}})T_s. \tag{3}$$

In this paper, we assume that the TDOA is an integer multiple of samples. Fractional TDOA values could be handled by comparing the sampling phase in the two receivers. Specifically, (2) is obtained by sampling the received signals $iT_s + \phi_{\rm ref}$ and $iT_s + \phi_{\rm pri}$, where the sampling phases $\phi \in [0, T_s)$ are adjusted by each receiver according to some standard sample timing algorithm (e.g., energy maximization). There will also in principle be a small timing offset $\tau_{\rm off}$ between the clocks at the two receivers, and if there is a sampling clock frequency offset (ScFO), then $\tau_{\rm off}$ will gradually change, typically as a random walk. Thus, the TDOA accounting for all of these effects is

$$T = (\delta_{\rm pri} - \delta_{\rm ref})T_s + \phi_{\rm pri} - \phi_{\rm ref} + \tau_{\rm off} \tag{4}$$

where everything but $\tau_{\rm off}$ is known. In the navigation problem, in which there are only two receivers, the offset $\tau_{\rm off}$ can be included in the parameters to be solved for; i.e., after obtaining the various TDOA estimates, the problem is to jointly estimate two or three position coordinates and $\tau_{\rm off}$. In the source localization problem (which uses many receivers and hence could have a different timing offset for each receiver), the receivers must be synchronous to some accuracy for *any* TDOA-based method to work. A total offset of τ seconds translates to $c\tau$ meters (where c is the speed of light), hence the positioning accuracy requirements govern the largest acceptable time offset, and the receivers will need to coordinate in order to ensure the clocks are synchronous to that accuracy.

III. TDOA Computation

A. Traditional, Centralized Computation

The traditional method of computing TDOAs involves a correlation of the raw data received at the primary and reference receivers. The reference receiver retransmits a copy of K samples it receives, $y_{\rm ref}(k)$, to the primary receiver. Then the latter performs a correlation:

$$R_y(d) = \sum_{k=1}^{K} y_{\rm ref}(k) y_{\rm pri}^*(k+d). \tag{5}$$

The primary must compute (5) for all anticipated valid ranges of the block arrival time difference, say $-DM \le d \le DM$, i.e., about $2DM$ samples, or $2D$ blocks. Then the TDOA can be computed as

$$\begin{aligned} \delta &= \arg \max_{-DM \le d \le DM} \mathcal{R}\{R_y(d)\} \\ \widehat{\rm TDOA} &= \delta T_s \end{aligned} \tag{6}$$

where $\mathcal{R}\{\cdot\}$ is the real operator and T_s is the sample period. Throughout the remainder of the paper, we refer to this as the traditional, centralized approach, since all of the raw data must be retransmitted to a central location for processing.

B. Proposed Decentralized Computation

The proposed TDOA computation is a two-step process:

S1) (block boundaries): The reference uses the CP to locate the block boundaries within the signal that it receives. Simultaneously and independently, the primary performs the same task on its received signal.

S2) (feature extraction): The reference and the primary each compute a single, scalar statistical feature from each block. The reference transmits the feature values and boundary times of the associated blocks to the primary, which then correlates the sets of feature values in order to line them up.

The first step is a fairly common method of blind (noncooperative) block synchronization [30]. In conventional communications applications, block synchronization must be performed in order to successfully demodulate the data. However, we perform the same task here in order to transform the TDOA computation from the time scale of samples to the time scale of blocks.

Note that S1) is what makes the proposed method specific to OFDM—for non-block-based methods, there would be no way to predefine times at which one could measure features. By blindly estimating the locations of the block boundaries, the two receivers can agree upon the times to calculate the features. An alternative approach could be to asynchronously look for particular statistical features, and then share the times of those features (rather than the proposed approach of sharing values of features at specific times). However, this approach may be sensitive to noise, e.g., if the feature is the occurrence of a large-amplitude spike or something similar.

For clarity of presentation, we review the blind block synchronization method of [30] here, but the novel work lies primarily in S2), which we will discuss later in this section. Given a received block, the maximum likelihood estimate of the block boundaries is given by [30]

$$\hat{\delta}_{\rm ML,rx} = \arg \max_{0 \le m \le M-1} \mathcal{R}\left\{\gamma(m) - \left(\frac{\sigma_x^2}{\sigma_x^2 + \sigma_{\rm rx}^2}\right)\Phi(m)\right\} \tag{7}$$

where the subscript "*rx*" will be used throughout to generically denote either the reference or the primary, and where

$$\gamma(m) = \sum_{i=m+1}^{m+\nu} y_{\rm rx}(i) y_{\rm rx}^*(i+N) \tag{8}$$

$$\Phi(m) = \frac{1}{2}\sum_{i=m+1}^{m+\nu} \left(|y_{\rm rx}(i)|^2 + |y_{\rm rx}(i+N)|^2\right) \tag{9}$$

denote the prospective CP to end-of-symbol correlation and the power in the CP and the end-of-symbol. Note that [30] also assumes the presence of a carrier frequency offset (CFO) which complicates the equations, whereas we do not for simplicity. Thus, (7) is a simplification of [30, eq. (12)] when the CFO $\epsilon = 0$.

As opposed to [30], in our work we average over many blocks. This causes the power term $\Phi(m)$ to be nearly constant as a function of m, hence we omit it. Including this averaging and approximation, the estimate of the block boundaries becomes

$$\hat{\delta}_{\rm ML,rx} \cong \arg \max_{0 \le m \le M-1} \mathcal{R}\{\gamma_{\rm avg}(m)\} \tag{10}$$

$$\gamma_{\text{avg}}(m) = \sum_{k=0}^{L-1} \sum_{i=m+1}^{m+\nu} y_{\text{rx}}(Mk+i) y_{\text{rx}}^*(Mk+i+N) \quad (11)$$

where L is the number of blocks included in the averaging. Note that if our primary goal is to reduce the bandwidth between the reference and the primary, each sensor can use an arbitrarily large L (subject to internal complexity constraints) without affecting this bandwidth.

Unfortunately, there is an ambiguity in the estimate of (10), since at this point we cannot tell one block from another—we simply know where the boundaries are. In a standard communications application, this is not a problem, since synchronization is only performed to be able to demodulate the data, and the value of the propagation delay is not of interest in and of itself. However, for TDOA computation, we need to know the value of the difference of two propagation delays, so we must move on to the second step of the process described at the start of this section [S2 (feature extraction)].

Given the block boundaries, we parse the received signals into blocks, with the kth block given by

$$\mathbf{y}_{\text{rx}}(k) = \begin{bmatrix} y_{\text{rx}}(Mk+1+\hat{\delta}_{\text{ML,rx}}) \\ \vdots \\ y_{\text{rx}}(Mk+M+\hat{\delta}_{\text{ML,rx}}) \end{bmatrix}. \quad (12)$$

The task now is to compute some scalar feature for this block, which can be used to label it and discriminate it from other arbitrary received blocks. Thus, a desirable feature will vary significantly from block to block. It should depend on the underlying signal as much as possible and on the noise as little as possible. Some of the features we considered include the first four normalized central moments (mean, variance, skewness, and kurtosis)

$$\mu_{\text{rx}}(k) = \frac{1}{M} \sum_{i=1}^{M} [\mathbf{y}_{\text{rx}}(k)]_i \quad (13)$$

$$\sigma_{\text{rx}}^2(k) = \frac{1}{M} \|\mathbf{y}_{\text{rx}}(k) - \mu_{\text{rx}}(k) \cdot \mathbf{1}\|_2^2 \quad (14)$$

$$\lambda_{\text{rx}}(k) = \frac{1}{\sigma_{\text{rx}}^3(k)} \frac{1}{M} \|\mathbf{y}_{\text{rx}}(k) - \mu_{\text{rx}}(k) \cdot \mathbf{1}\|_3^3 \quad (15)$$

$$\xi_{\text{rx}}(k) = \frac{1}{\sigma_{\text{rx}}^4(k)} \frac{1}{M} \|\mathbf{y}_{\text{rx}}(k) - \mu_{\text{rx}}(k) \cdot \mathbf{1}\|_4^4, \quad (16)$$

the "mini-mean"

$$\overline{\mu}_{\text{rx}}(k) = \frac{1}{2\nu} \left(\sum_{i=1}^{\nu} [\mathbf{y}_{\text{rx}}(k)]_i + \sum_{i=N+1}^{M} [\mathbf{y}_{\text{rx}}(k)]_i \right), \quad (17)$$

the average symbol's phase

$$\Phi_{\text{rx}}(k) = \angle\{\mu_{\text{rx}}(k)\}, \quad (18)$$

and the peak-to-average power ratio

$$\text{PAPR}_{\text{rx}}(k) = \frac{\|\mathbf{y}_{\text{rx}}(k)\|_\infty^2}{\|\mathbf{y}_{\text{rx}}(k)\|_2^2} \quad (19)$$

where $[\cdot]_i$ refers to the ith element of a vector and $\mathbf{1}$ is an appropriately-sized column vector of ones. Other features were considered, such as the root-mean-squared signal (preserving phase), the standard deviation, and various frequency domain features; for a full list, see [31]. We found that the mini-mean feature yielded the best performance, hence the analytic and simulation results will focus on the mean and mini-mean features, but the notation will be left in a general form to allow for alternative features. To see the performance of other features, see [31]. Also note that the features in (13)–(19) are not an exhaustive list, merely those which appeared promising and were computationally simply to compute. The authors know of no systematic way to derive other features that may perform better, but certainly other features could be proposed.

The statistical features are sample averages of small amounts of data, hence they vary from block to block, which is what allows for detectability of the TDOA. For example, consider three blocks of random binary data, $[-1, 1, 1, -1]$, $[1, 1, -1, 1]$, and $[1, -1, -1, -1]$. The "mean" features of these blocks are $0, 1/4, -1/4$. One can search for this pattern of three means rather than searching for the original pattern of 12 bits, which reduces the data required for the correlation. This is only enabled when the data has a block structure, as in multicarrier systems.

The reference calculates the value of a particular feature for each of K blocks, then transmits these K values and its estimate of $\hat{\delta}_{\text{ref}}$ to the primary. Assuming complex-valued features, $2K+1$ real numbers must be transmitted from the reference to the primary each time the TDOA estimate is updated.

Given the data from the reference, the primary can compute and maximize the covariance of the features. Generically denoting the feature values as $f_{\text{ref}}(k)$ and $f_{\text{pri}}(k)$, the primary computes

$$R_f(d) = \sum_{k=1}^{K} (f_{\text{ref}}(k) - f_{\text{ref}}^{\text{avg}}(1)) \times \left(f_{\text{pri}}(k+d) - f_{\text{pri}}^{\text{avg}}(1+d) \right)^* \quad (20)$$

where

$$f_{\text{pri}}^{\text{avg}}(j) = \frac{1}{K} \sum_{k=j}^{j+K-1} f_{\text{pri}}(k) \quad (21)$$

and similarly for the reference. The primary must compute (20) for all anticipated valid ranges of the block arrival time difference, say $-D \leq d \leq D$. Thus, while the reference computes the feature values for K blocks, the primary must compute them for $K + 2D$ blocks. Once (20) has been computed over this range, the TDOA can be computed as

$$\begin{aligned} \Delta &= \arg \max_{-D \leq d \leq D} \mathcal{R}\{R_f(d)\} \\ \delta &= \hat{\delta}_{\text{pri}} - \hat{\delta}_{\text{ref}} \\ \widehat{\text{TDOA}} &= (\delta + M\Delta) T_s \end{aligned} \quad (22)$$

where $\mathcal{R}\{\cdot\}$ is the real operator; δ is the offset in samples, modulo M; Δ is the offset in blocks, which accounts for the modulo M ambiguity; and T_s is the sample period. Again, we assume baud rate sampling for simplicity of analysis, but this procedure could be extended to the oversampled case by increasing M, N, and ν, and decreasing T_s by the oversampling factor, leaving the rest of the procedure unchanged.

C. Position Estimation and Tracking

Once the TDOAs have been determined, either through the traditional centralized or the proposed decentralized processes, then there are various methods to estimate and track the source position [27]–[29]. These methods can help mitigate the errors in the TDOAs due to multipath. For example, as opposed to most other methods of geolocation, in [27], the variances of the TDOA estimates are not assumed to be known, since multipath can increase them; and in [28], a Kalman filter is used to track inconsistencies between the TDOA estimates and the position estimates in the form of biases in the TDOAs. If available, training can also be used to reduce errors due to multipath and/or non-line-of-sight (NLOS) errors [24]. Since this paper focuses on the TDOA estimation step rather than the subsequent geolocation or navigation step, we do not pursue these approaches further. However, evaluating our work in the context of various geolocation algorithms may form a starting point for further work.

IV. Bandwidth and Complexity

In this section, we discuss what resources are available and how much of each is used. This includes a discussion of how many blocks K can be used in the feature correlator, the bandwidth between the reference and the primary, the computational complexity at the primary, the time required to gather enough data for a position estimation, and the size of the geographical area to be searched.

The parameters L and K (the number of blocks used in S1 and S2, respectively) are of great importance because increasing them will improve the estimate of the TDOA, as will be quantified in the next two sections. However, if the primary or the transmitter is moving quickly, the true value of the TDOA will change over time, and if too many blocks are used, the TDOA will not be approximately constant within the estimation interval. Assume that the reference is stationary and that either the primary or the transmitter is moving at a velocity v. The total length of the estimation interval in (20) is KMT_s seconds (here, K could equivalently be replaced by L), and during this time the primary will move KMT_sv meters. Depending on the geometry, the maximum change in propagation time from the transmitter to the primary or the reference is $\pm KMT_sv/c$ seconds (each), where c is the speed of light. The worst case scenario is such that the transmitter is colinear with the two sensors and is moving directly towards one of them and directly away from the other. We would like the total change in TDOA to be much less than the resolution of our sampling, i.e.,

$$2KMT_s\frac{v}{c} \ll T_s \tag{23}$$

which bounds K by

$$KM \ll \frac{1}{2}\frac{c}{v}. \tag{24}$$

If the primary or the transmitter is on an aircraft travelling at the speed of sound, $v = 343$ m/s (or about 767 mph), then $KM \ll 437\,500$. For a block size of $M = 80$ as used in our simulations, this means that K (or L) $\ll$5500 blocks can be used. If $M = 2560$ (among the largest used in existing OFDM systems), then K (or L) $\ll$170 blocks can be used. Of course, this is all for a worst case geometry and a very high velocity, so in practice more blocks may be used. On the other hand, if we oversample, we reduce the resolution requirement on the right-hand side of (23) without changing the product MT_s on the left-hand side of (23), hence the upper bound on K or L must be reduced.

The bandwidth between the reference and the primary should be as small as possible. For scalability of comparison, we will evaluate the reference-to-primary bandwidth as compared to the bandwidth used by the transmitter, rather than in an absolute sense. The transmitter transmits M complex samples per block. The reference transmits one feature value per block, and it may be real or complex. Assuming a complex-valued feature, the bandwidth ratio is

$$\frac{\mathrm{BW}_{\mathrm{ref}\to\mathrm{pri}}}{\mathrm{BW}_{\mathrm{tx}}} = \frac{1}{M}. \tag{25}$$

Typical values of M range from 80 to 2560, hence large savings are possible. However, as seen in the next section, if the centralized approach is used, the target performance may be reached by transmitting fewer blocks, and when that is factored in, the total bandwidth savings of our approach is a factor of 2 to 3. On the other hand, once an initial position estimate is determined and we are in a tracking environment, our "step 2" (which, of the two steps, is the step that typically causes any errors) is no longer necessary, and the proposed approach also does not require many blocks to maintain a target accuracy. Thus, our approach leads to a bandwidth savings of at least a factor of 2–3, and much more when in a tracking situation.

At the primary, the computational complexity of the proposed approach is dominated by three contributions:

- computation of $\{\gamma_{\mathrm{avg}}(m), 0 \le m \le M-1\}$;
- computation of $\{f_{\mathrm{pri}}(k), 1 \le k \le K\}$;
- and computation of $\{R_f(d), -D \le d \le D\}$.

We will only evaluate the complexity for the "mini-mean" feature, since it yielded by far the best performance. (This can be verified by noting that the "mean" feature was shown to outperform all other features except the "mini-mean" in [31], and the theoretical analysis in the next section shows that the "mini-mean" should be slightly superior to the "mean.")

First consider computation of $\gamma_{\mathrm{avg}}(m)$. It is a sum of L dot products of a pair of windows that slides with m. Thus, for the first value of m, $L\nu$ complex multiplies and additions are needed. However, as m is incremented, each dot product can be updated by appending and removing one term from each dot product. The elements to be removed have already been computed, hence only a total of L complex multiplies and additions are needed for each additional value of m. Thus, in total, computing $\{\gamma_{\mathrm{avg}}(m)\}$ requires approximately $L(M+\nu)$ complex multiplies and additions (each). Approximately LM word of memory are needed to store the data, although this could be reduced to approximately $3M$ words by performing the computations block-by-block rather than in a single batch process.

The complexity of the feature computation depends on the feature. The mini-mean requires a total of about $2\nu K$ complex additions. (Note that in practice we do not actually apply constant scale factors such as $1/M$ since they scale the signal and noise components equally.) K words of memory are needed to store the result.

The final correlation step requires computing $f_{\mathrm{ref}}^{\mathrm{avg}}$ and $f_{\mathrm{pri}}^{\mathrm{avg}}$, which are of negligible complexity. For each value of d, computing $R_f(d)$ requires $2K$ subtractions followed by K multiplies, for a total of about $2DK$ complex multiplies and additions, with $2D$ memory words to store R_f. In total, the computational complexity is approximately by $L(M+\nu)+2KD$ complex multiplies and $L(M+\nu)+2K(D+\nu)$ additions, computed over the span of KM samples of the source data; and $3M+K+2D$ words of memory are needed.

Now compare this complexity to the full, centralized cross-correlation approach, which does not exploit the OFDM structure. If the TDOA estimate ranges over $2D$ blocks, we must compute the cross-correlation for $2DM$ values of the correlation lag (in samples), using $2DM$ memory words to store the result. If the two sensors share K blocks of data (i.e., KM samples of data), each lag in the cross correlation is a length KM dot product, hence the total complexity would be $2KM^2D$ complex multiplies and additions, and $2DM$ memory words. However, a direct numerical comparison is difficult because the proposed approach and the standard approach need not use the same amount of data for comparable performance, and the complexity of the proposed approach is highly dependent on the transmission standard via the parameter M.

In terms of actual time spent to obtain a position estimate, the proposed method requires KMT_s seconds. For IEEE 802.11a, for example, $MT_s = 4\ \mu$s, and in digital video broadcast, MT_s ranges from 10 μs to 280 μs. Thus, for $K = 1000$ blocks, data acquisition time would range from 4 to 280 ms.

In order to define a search space for the feature correlation maximization, we assume that the unknown TDOA will fall into some range of $[-D, D]$ blocks, corresponding to a search space of $2cDMT_s$ meters. In our simulations, we assume $D = 100$. For the systems discussed in the previous paragraph, this corresponds to 240 to 16 800 km. Assuming *a priori* knowledge that the position is in a sphere of 240 km is reasonable, and in fact in most cases D could be reduced to $D = 10$, which would improve the performance of the simulations considerably. However, in order to not be restrictive, we will assume $D = 100$. Also note that in a tracking situation (after initial acquisition), it is likely that D will become less than 1, i.e., a fraction of a block. Then the decentralized approach does not need to continue transmitting feature values, just the times of the block boundaries; whereas the centralized approach must still continue to perform the correlation, since it operates at the sample level and an ambiguity of a fraction of a block is still many samples.

V. Analysis

In this section, we theoretically analyze the performance of the mean and mini-mean features, which led to the best performance. The performance metric will be P_e, the probability of error in the estimate of Δ in (22). This is essentially equivalent to the probability of making a TDOA error, since L can be chosen large enough to make an error in δ far less likely than an error in Δ. For simplicity of notation, in this section we assume that the true TDOA is zero. We also omit scale factors of $1/K$ since they scale the signal and noise components equally.

The "mean" features are computed as

$$f_{\mathrm{ref}}(k) = \overbrace{\frac{1}{M}\sum_{i=1}^{M} x(Mk+i)}^{X(k)} + \overbrace{\frac{1}{M}\sum_{i=1}^{M} n_{\mathrm{ref}}(Mk+i)}^{N_{\mathrm{ref}}(k)}$$
$$f_{\mathrm{pri}}(k) = \frac{1}{M}\sum_{i=1}^{M} x(Mk+i) + \underbrace{\frac{1}{M}\sum_{i=1}^{M} n_{\mathrm{pri}}(Mk+i)}_{N_{\mathrm{pri}}(k)}.$$

By the central limit theorem, $X(K), N_{\mathrm{ref}}(k)$, and $N_{\mathrm{pri}}(k)$ are approximately Gaussian with zero mean and variance

$$\sigma_X^2 = \frac{M+2\nu}{M^2}\sigma_x^2 = \frac{1+2\nu/M}{M}\sigma_x^2 \tag{26}$$
$$\sigma_{N,\mathrm{ref}}^2 = \frac{1}{M}\sigma_{\mathrm{ref}}^2 \tag{27}$$
$$\sigma_{N,\mathrm{pri}}^2 = \frac{1}{M}\sigma_{\mathrm{pri}}^2 \tag{28}$$

where the term 2 ν in the numerator of σ_X^2 accounts for the correlation of the last ν samples of the block with the CP.

The "mini-mean" feature is almost identical to the mean. However, only the first ν and the last ν terms are included in the averaging, and these are precisely the terms which are correlated with each other. Thus, for the mini-mean feature, we have

$$\sigma_X^2 = \frac{2\nu+2\nu}{(2\nu)^2}\sigma_x^2 = \frac{2}{2\nu}\sigma_x^2 \tag{29}$$
$$\sigma_{N,\mathrm{ref}}^2 = \frac{1}{2\nu}\sigma_{\mathrm{ref}}^2 \tag{30}$$
$$\sigma_{N,\mathrm{pri}}^2 = \frac{1}{2\nu}\sigma_{\mathrm{pri}}^2. \tag{31}$$

Comparing the mini-mean to the mean, the "feature SNR" σ_X^2/σ_N^2 has improved by a factor of $2/(1+2\nu/M)$, which is about 1.4 to 2 for typical OFDM systems. This improvement was the motivation for selecting the mini-mean as a feature, and the rest of the analysis will be performed in terms of the mini-mean alone.

Since we have $\mathbf{E}[f(k)] = 0$ for this feature, the covariance of the features reduces to a correlation

$$\begin{aligned} R_f(d) &= \sum_{k=1}^{K} f_{\mathrm{ref}}(k) f_{\mathrm{pri}}^*(k+d) \\ &= \sum_k X(k)X^*(k+d) + \sum_k X(k)N_{\mathrm{pri}}^*(k+d) \\ &\quad + \sum_k N_{\mathrm{ref}}(k)X^*(k+d) \\ &\quad + \sum_k N_{\mathrm{ref}}(k)N_{\mathrm{pri}}^*(k+d). \end{aligned} \tag{32}$$

The next task is to determine the mean and the variance of $R_f(d)$ as functions of d. The mean is straightforward, since the last three terms in (32) are zero mean:

$$\mathbf{E}[R_f(d)] = \begin{cases} K\sigma_X^2, & d=0 \\ 0, & d \neq 0 \end{cases}. \tag{33}$$

To compute the variance, we will first compute the second moment.

$$\mathbf{E}\left[|R_f(d)|^2\right] = \sum_{k=1}^{K}\sum_{l=1}^{K} f_{\mathrm{ref}}(k) f^*_{\mathrm{pri}}(k+d) f_{\mathrm{ref}}(l) f^*_{\mathrm{pri}}(l+d). \tag{34}$$

Expanding (34) as in (32) yields 16 terms, only four of which are nonzero:

$$\begin{aligned}\mathbf{E}&\left[|R_f(d)|^2\right]\\ &= \sum_{k=1}^{K}\sum_{l=1}^{K}\mathbf{E}[X(k)X^*(k+d)X^*(l)X(l+d)]\\ &\quad+\sum_{k=1}^{K}\sum_{l=1}^{K}\mathbf{E}[X(k)X^*(l)]\mathbf{E}[N^*_{\mathrm{pri}}(k+d)N_{\mathrm{pri}}(l+d)]\\ &\quad+\sum_{k=1}^{K}\sum_{l=1}^{K}\mathbf{E}[X^*(k+d)X(l+d)]\mathbf{E}\left[N_{\mathrm{ref}}(k)N^*_{\mathrm{ref}}(l)\right]\\ &\quad+\sum_{k=1}^{K}\sum_{l=1}^{K}\mathbf{E}[N_{\mathrm{ref}}(k)N^*_{\mathrm{ref}}(l)]\,\mathbf{E}\left[N^*_{\mathrm{pri}}(k+d)N_{\mathrm{pri}}(l+d)\right].\end{aligned} \tag{35}$$

The last three terms of (35) are simple. For the first term, we must consider the $d=0$ and $d\neq 0$ cases separately. For $d=0$, there will be K terms within the double summation in which $k=l$ and hence all four factors have the same index, and $K(K-1)$ terms in which the first two indexes are the same but are different from the last two indices. Thus, we have

$$\begin{aligned}\sum_{k=1}^{K}\sum_{l=1}^{K}&\mathbf{E}[X(k)X^*(k+d)X^*(l)X(l+d)]|_{d=0}\\ &= K\mathbf{E}\left[|X(k)|^4\right] + K(K-1)\left(\mathbf{E}\left[|X(k)|^2\right]\right)^2\\ &= K(K+1)\sigma_X^4.\end{aligned} \tag{36}$$

(Note that herein we are assuming complex-valued data. For real-valued data, the last line above would need to change slightly to $K(K+2)\sigma_X^2$ to account for the difference in kurtosis between real and complex Gaussian random variables, but the rest of the derivation would remain unchanged.) For $d\neq 0$, the only way for an even number of indexes to line up is if $k=l$, and there are K such occurrences. Thus, we have

$$\begin{aligned}\sum_{k=1}^{K}\sum_{l=1}^{K}&\mathbf{E}[X(k)X^*(k+d)X^*(l)X(l+d)]|_{d\neq 0}\\ &= K\left(\mathbf{E}\left[|X(k)|^2\right]\right)^2\\ &= K\sigma_X^4.\end{aligned} \tag{37}$$

Accounting for the last three terms in (35) and noting that the variance of $R_f(d)$ is the second moment from (35) minus the square of the first moment from (33), we have

$$\begin{aligned}\mathrm{VAR}[R_f(d)] &= K\left(\sigma_X^4 + \sigma_X^2\sigma_{N,\mathrm{ref}}^2\right.\\ &\qquad\left.+\sigma_X^2\sigma_{N,\mathrm{pri}}^2 + \sigma_{N,\mathrm{ref}}^2\sigma_{N,\mathrm{pri}}^2\right)\\ &= K\left(\sigma_X^2+\sigma_{N,\mathrm{ref}}^2\right)\left(\sigma_X^2+\sigma_{N,\mathrm{pri}}^2\right).\end{aligned} \tag{38}$$

In the special case $\sigma_{N,\mathrm{ref}}^2 = \sigma_{N,\mathrm{pri}}^2 \triangleq \sigma_N^2$, this reduces to

$$\mathrm{VAR}[R_f(d)] = K\left(\sigma_X^2+\sigma_N^2\right)^2. \tag{39}$$

Together, (33) and (39) characterize the mean and variance of the feature correlation.

The mean and variance can be used to obtain a "correlation SNR" as follows. We are looking at $R_f(d)$ to locate a large, real-valued spike. Thus, we can throw away the imaginary part, and the real-valued part of the function will have half the variance. The "correlation SNR" will shortly be shown to explicitly govern the probability of error, and we define it as the ratio of the difference of the peak to off-peak means to the standard deviation of the real part

$$\gamma = \frac{K\sigma_X^2}{\sqrt{K/2}\left(\sigma_X^2+\sigma_N^2\right)}. \tag{40}$$

Substituting from (29)–(31) and simplifying

$$\begin{aligned}\gamma &= \sqrt{2K}\frac{2\sigma_x^2}{2\sigma_x^2+\sigma_{\mathrm{rx}}^2}\\ &= \sqrt{2K}\frac{\mathrm{SNR}}{\mathrm{SNR}+\frac{1}{2}}.\end{aligned} \tag{41}$$

Note that we have various SNR-like terms in this paper. The unqualified term "SNR" is simply $\sigma_x^2/\sigma_{\mathrm{ref}}^2$ or $\sigma_x^2/\sigma_{\mathrm{pri}}^2$, i.e., received signal power over received noise power. The term "feature SNR" is σ_X^2/σ_N^2, and it refers specifically to the powers of the signal and noise components of the features $f_{\mathrm{rx}}(k)$. Finally, the "correlation SNR" γ is a ratio of the powers of the signal and noise portions of the correlation function $R_f(d)$. Thus, when determining the probability of error in the feature correlation, the "correlation SNR" γ will be the governing factor, as we now derive. Also note that the correlation SNR is proportional to the square root of the number of blocks. For large SNR, γ becomes flat, and for small SNR, γ is roughly proportional to the SNR.

In order to determine the probability of error, define the shorthand $R_d \triangleq \mathcal{R}\{R_f(d)\}$. We will approximate R_d as a set of independent jointly Gaussian random variables, with means and variances as determined above. The jointly Gaussian approximation is justified by the central limit theorem for vectors [32], at least for large K. The independence assumption is also justified for large K since R_d are jointly Gaussian and can be shown to have a correlation coefficient of zero. This requires following a procedure similar to (35), except with two different values of d, and is omitted here since it is fairly similar. We will validate these approximations by comparing the theoretical results to simulations in Section VI. Under these approximations, the probability of *not* making an error in the estimate of Δ is simply the probability that no value of $\{R_d, d\neq 0\}$ exceeds R_0,

$$1-P_e = P\left(\bigcap_{d\in\mathcal{D}} R_d < R_0\right) \tag{42}$$

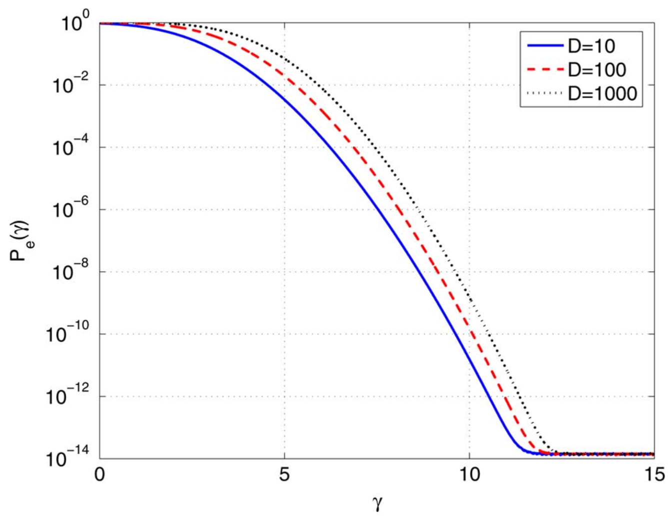

Fig. 4. Probability of error in the TDOA estimate as a function of the "correlation SNR" γ.

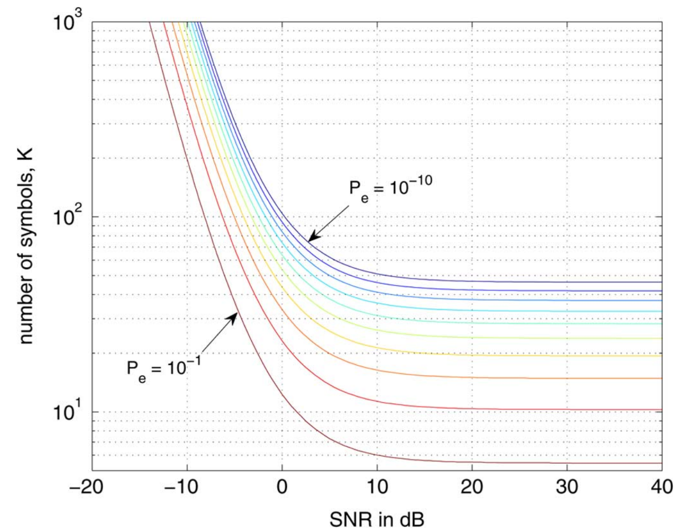

Fig. 5. Contours of the theoretical probability of error as a function of the SNR and the number of symbols K, for the proposed partially decentralized method. The search range of the TDOA was over $D = 10$ symbols of $M = 80$ samples each. The contour levels are spaced by orders of magnitude.

where $\mathcal{D} = \{\pm 1, \ldots, \pm D\}$. Using the independence of R_m and R_n, the probability can be written in integral form as

$$1 - P_e = \int_{-\infty}^{\infty} \prod_{d \in \mathcal{D}} \left[\int_{-\infty}^{R_0} p\left(R_d\right) dR_d \right] p(R_0)\, dR_0$$
$$= \int_{-\infty}^{\infty} \left[\int_{-\infty}^{R_0} p(R_1)\, dR_1 \right]^{2D} p\left(R_0\right) dR_0 \quad (43)$$

where the last line follows from the identical distributions of $\{R_d, d \neq 0\}$. Using the Gaussian approximation

$$R_0 \sim \mathcal{N}\left(m_R, \frac{1}{2}\sigma_R^2\right), \quad (44)$$
$$R_1 \sim \mathcal{N}\left(0, \frac{1}{2}\sigma_R^2\right) \quad (45)$$

where m_R and σ_R^2 are as given in (33) and (39). After changes of variables $R_0 \to x$ and $R_1 \to y$ to normalize to zero mean and unit variance, we have

$$1 - P_e = \int_{-\infty}^{\infty} \left[\int_{-\infty}^{x+\gamma} p(y)\, dy \right]^{2D} p(x)\, dx \quad (46)$$

where $\gamma = m_R/\sigma_R$ as in (41). Substituting in normalized Gaussian PDFs for x and y

$$P_e = 1 - \frac{1}{\sqrt{2\pi}} \int_{-\infty}^{\infty} \left[1 - Q(x+\gamma)\right]^{2D} e^{-x^2/2}\, dx. \quad (47)$$

This is a fairly easy-to-compute function of D and the threshold γ, which in turn is a simple function of K and the SNR via (41).

Fig. 4 shows the probability of error from (47) versus γ for $D = 10$, 100, and 1000. Other features besides the mean may have different functional dependencies between the SNR, K, and γ, but Fig. 4 is independent of the feature once γ has been determined. If at the outset you do not have a good estimate of the position, you will have to search using a large value of D. Fig. 4 shows that every order of magnitude increase in D (which is roughly an order of magnitude increase in each dimension of the search space of the TDOA estimator) corresponds to approximately an order of magnitude increase in the probability of error.

Fig. 5 shows contours of the probability of error from (41) and (47) for a range of K and SNR values, for $D = 10$. (For the parameters used in our simulations, this equates to assuming that the transmitter is within an area of diameter $cT_sMD = 12$ km.) This shows a curious effect stemming from the dependence of γ on K and the SNR, via (41). For low SNR, $\gamma \propto \sqrt{K}\mathrm{SNR}$, and for high SNR, $\gamma \propto \sqrt{K}$. Thus, in the low SNR region, γ can be increased either by increasing K or the SNR, but in the high SNR region, if K is fixed, then γ cannot be changed even if the SNR is further increased. The upshot of this is that in Fig. 5, we see that for $K = 10$, it is simply impossible to achieve $P_e < 0.05$ even as the SNR goes to infinity. This explains some of the simulation results to be discussed in Section VI.

In order to compare the proposed approach to the centralized approach, we can develop a plot similar to Fig. 5 as follows. Assume a total TDOA ambiguity of D blocks, or MD samples. Let K be the total amount of data transmitted from the reference to the primary; for the decentralized approach, this was the number of blocks worth of features, and for the centralized approach it is the number of samples of the received sequence. Then, in the centralized approach, the TDOA is computed as

$$R_y(d) = \sum_{k=1}^{K} y_{\mathrm{ref}}(k) y_{\mathrm{pri}}^*(k+d) \quad (48)$$
$$\widehat{\mathrm{TDOA}} = T_s \cdot \arg \max_{-MD \le d \le MD} \mathcal{R}\{R_y(d)\} \quad (49)$$

which is similar to but distinct from (22). The rest of the analysis is fairly similar to that of the feature correlation, with one major exception: while the feature values are uncorrelated from block to block, the samples of the received signal are not uncorrelated over time, due to the presence of the CP. This correlation creates two small side peaks in $R_y(d)$ at $d = \pm\nu$. Omitting the

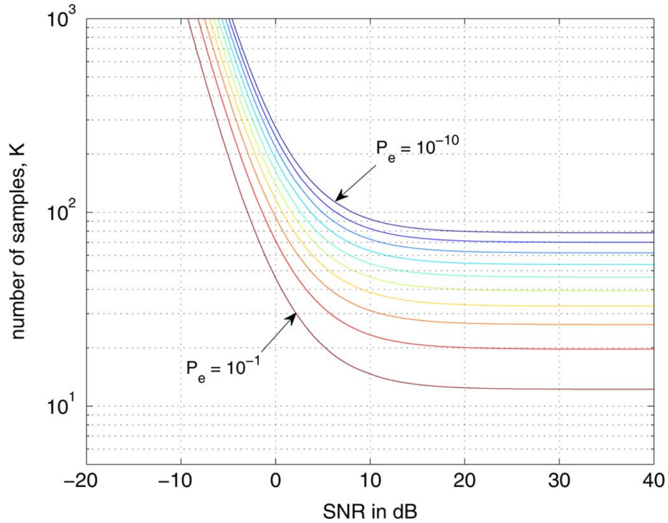

Fig. 6. Contours of the theoretical probability of error as a function of the SNR and the number of samples K, for the centralized method. The search range of the TDOA was over $D = 10$ symbols of $M = 80$ samples each. The contour levels are spaced by orders of magnitude.

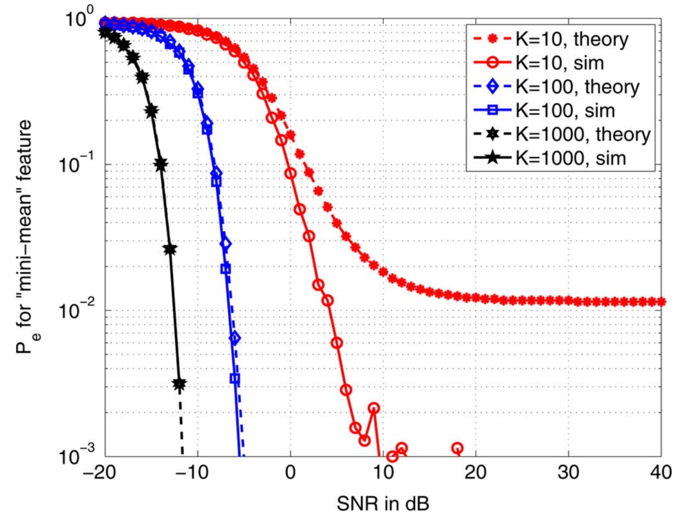

Fig. 7. Comparison of theoretical and simulated probability of synchronization error versus SNR, for the "mini-mean" feature.

details, which are similar to but slightly more involved than for the proposed approach, we obtain a probability of error of

$$P_e^{\text{central}} = 1 - \frac{1}{\sqrt{2\pi}} \int_{-\infty}^{\infty} [1 - Q(\alpha x + \gamma_1)]^{2D-2} \times [1 - Q(\alpha x + \gamma_2)]^2 e^{-x^2/2}\, dx \tag{50}$$

where

$$\alpha = \sqrt{1 + \frac{2\nu}{M}\left(\frac{\text{SNR}}{\text{SNR}+1}\right)^2} \tag{51}$$

$$\gamma_1 = \sqrt{2K}\frac{\text{SNR}}{\text{SNR}+1} \tag{52}$$

$$\gamma_2 = \left(1 - \frac{\nu}{M}\right)\gamma_1. \tag{53}$$

(Here, γ_1 and γ_2 are analogous to the correlation SNR γ, although for the centralized approach the signal strength varies within $R_f(d)$ due to the presence of the CP, hence the correlation SNR takes on two different values at different locations.) A plot of the probability of error from (50) is given in Fig. 6.

A direct comparison between the centralized method (Fig. 6) and the proposed partially decentralized method (Fig. 5) is difficult. We can hold any two of the SNR, the amount of data K, and the probability of error constant and compare the third. For example, at a 0.01% probability of error and $K = 100$, the decentralized approach can operate at an SNR of -2 dB, but the centralized approach operates at 1 dB, for a 3-dB gain. Or, at a 0.01% probability of error and an SNR of -5 dB, the decentralized approach requires $K = 250$ feature values but the centralized approach requires $K = 650$ samples. Finally, for $K = 50$ and an SNR of 10 dB, the decentralized approach has a probability of error of 3×10^{-9} and the centralized approach has a probability of error of 10^{-5}. Moreover, once the ambiguity has been resolved through the feature correlation and an initial position fix has been determined, tracking the position via the decentralized approach requires less bandwidth because the feature values no longer need to be transmitted, and the position can be tracked by simply comparing the reception times of the block boundary at the reference and the primary sensor, since it is unlikely that the TDOA would jump by an entire block of M samples between two successive position measurements; whereas the centralized method must still transmit signal values from the reference since it is not unlikely that the TDOA will change by several samples between two successive position measurements.

VI. Simulations

This section provides a performance analysis via simulations. The transmitter uses multicarrier modulation with an FFT size of $N = 64$, a CP length of $\nu = 16$, a block size of $M = 80$, and a bandwidth of 20 MHz ($T_s = 50$ ns) which are consistent with the IEEE 802.11a, HIPERLAN/2, and MMAC standards for wireless LANs. We also assumed $D = 10$ throughout, which assumes prior knowledge that the transmitter is within an area of diameter $cT_sMD = 12$ km. For simplicity, the noise powers are the same at both sensors, i.e., $\sigma_{\text{ref}}^2 = \sigma_{\text{pri}}^2$, hence the SNR at either sensor is $\text{SNR} = \sigma_x^2/\sigma_{\text{pri}}^2$.

A plot of the probability of correctly determining the overall TDOA is given in Fig. 7 for the mini-mean feature. Here, we used $L = 2000$ blocks to make step 2 the limiting factor in performance. Performance of the mean, variance, phase, and peak-to-average power ratio features was several decibels worse; and performance of the skewness and kurtosis was such that they are unusable. For the mini-mean, perfect synchronization is achieved 95% of the time at 10-dB SNR with only $K = 10$ blocks. If $K = 100$ blocks are available, perfect synchronization is almost always achieved at -3-dB SNR; and if $K = 1000$ blocks are available, perfect synchronization is almost always achieved at -10-dB SNR. The theoretical values agree with the simulated values very well, except for small amounts of data ($K = 10$), for which the central limit theorem based Gaussian approximation is of marginal validity.

The effect of varying the parameter L is shown in Fig. 8. The parameters are the same as in Fig. 7, except that the SNR was fixed to 0 dB and L was varied. Observe that the asymptotic

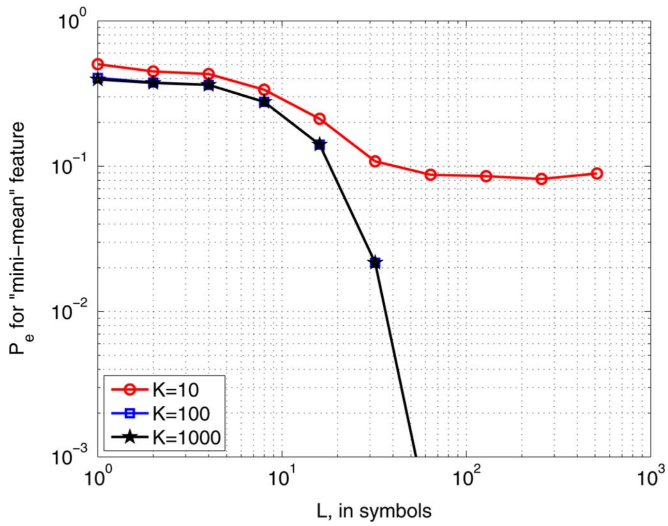

Fig. 8. Simulated probability of synchronization error as a function of number of blocks L in step 1, for the "mini-mean" feature. The SNR was 0 dB and D was 10. The "large L" performance of Fig. 7 is obtained for $L = 100$ or greater.

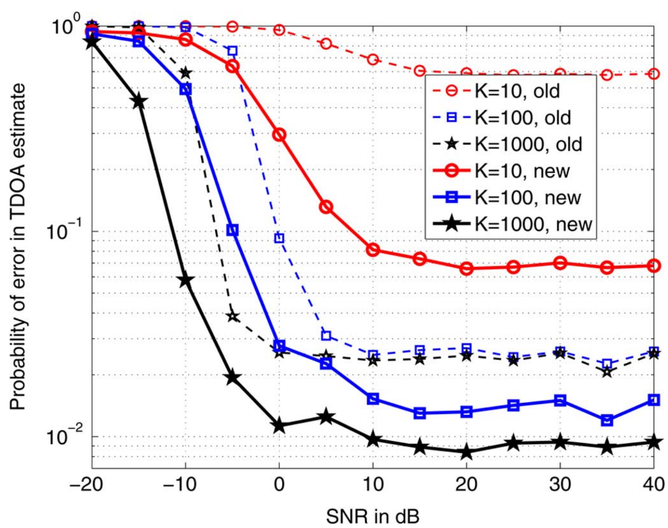

Fig. 9. Simulated probability of synchronization error versus SNR, in the presence of multipath. The channels each had a Ricean LOS path and a Rayleigh-fading path, and the two channels were different.

performance for large values of L is obtained for $L = 100$ or greater, hence L is not a significant limiting factor.

The effect of multipath is shown in Figs. 9 and 10. In the legends, "old" is the traditional centralized approach, and "new" is the proposed approach. The total bandwidth (i.e., K samples of communication) of the two approaches was equated, rather than equating performance and comparing bandwidth. Each channel had a Ricean LOS path with a variance -10 dB (relative to the LOS path's mean^2). In Fig. 9, the channels from the transmitter to the two receivers had Rayleigh fading NLOS paths at -5 dB (primary) and -7 dB (reference). In Fig. 10, the channels had Rayleigh fading NLOS paths at -6 dB, -10 dB, and -14 dB (primary), and -8 dB, -10 dB, and -14 dB (reference). The results in Figs. 9 and 10 are degraded compared to Fig. 7, although if the TDOA location estimator was used in conjunction with a Kalman filter for tracking, the performance would still be acceptable. For stronger multipath, it may be necessary to

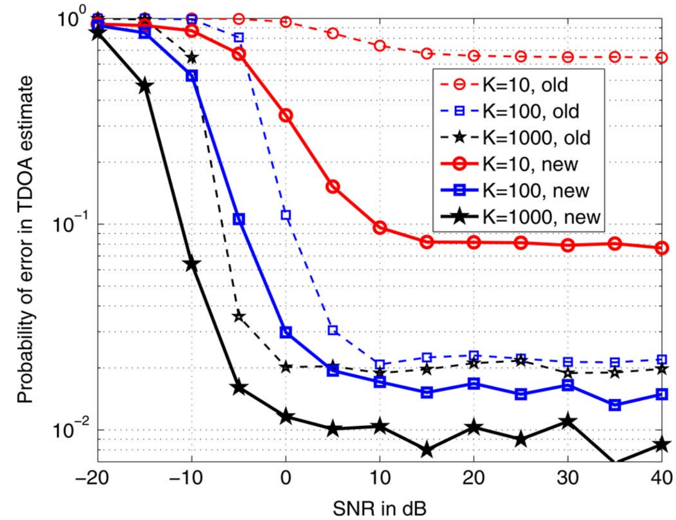

Fig. 10. Simulated probability of synchronization error versus SNR, in the presence of multipath. The channels each had a Ricean LOS path and three Rayleigh-fading paths, and the two channels were different.

use $K = 100$ or even $K = 1000$ to maintain performance, depending on the SNR.

If desired, the P_{error} results in this section could be lowered by combining several features into the correlator of (20). This would enable a tradeoff between the bandwidth used from the reference to the primary and the synchronization performance.

VII. Conclusion

We have shown that multicarrier modulation can be used to perform accurate TDOA computation with an SNR as low as -3 dB when 100 blocks are available. No training signal was required, although we did assume knowledge of the block structure of the transmitted signal. The only communication required between the reference and the primary for this level of performance was the transmission of 100 complex numbers and one integer over the course of the 100 block (8000 sample) time window, hence the bandwidth from the reference to the primary was almost two orders of magnitude smaller than the bandwidth of the signal of opportunity.

We analytically evaluated the performance of the proposed, partially decentralized approach and compared it to that of the standard centralized approach. For a given level of performance, the proposed approach requires two to three times less bandwidth; or from another point of view, it yields the same performance at 3–5 dB lower SNR for comparable bandwidths.

Future work will include investigating the effects of multipath, extending the analysis to the oversampled case, which would introduce correlation within the feature computation, and investigating methods of multipath mitigation. When training is available, the channel modelling and physics can be used to mitigate NLOS errors [24], but mutlipath mitigation is much more challenging in a blind environment.

References

[1] G. Sun, J. Chen, W. Guo, and K. J. R. Liu, "Signal processing techniques in network-aided positioning," *IEEE Signal Process. Mag.*, vol. 22, pp. 12–23, Jul. 2005.

[2] D. Blatt and A. O. Hero, III, "Energy-based sensor network source localization via projection onto convex sets," *IEEE Trans. Signal Process.*, vol. 54, no. 9, pp. 3614–3619, Sep. 2006.

[3] H. Wang and P. Chu, "Voice source localization for automatic camera pointing system in video conferencing," in *Proc. IEEE Int. Conf. Acoustics, Speech, Signal Processing*, Munich, Germany, Apr. 1997, vol. 1, pp. 187–190.

[4] T. K. S. Stephen, "Source localization using wireless sensor networks" Master's thesis, Naval Postgraduate School, Monterey, CA, Jun. 2006 [Online]. Available: http://handle.dtic.mil/100.2/ADA457683

[5] T. D. Hall, "Radiolocation using AM broadcast signals," Ph.D. dissertation, Massachusetts Ins. of Technology, Cambridge, MA, Sep. 2002.

[6] T. D. Hall, "Radiolocation using AM broadcast signals: The role of signal propagation irregularities," in *Proc. IEEE Position, Location, Navigation Symp. (PLANS)*, Monterey, CA, Apr. 2004, pp. 752–761.

[7] K. A. Fisher, "The navigation potential of signals of opportunity-based time difference of arrival measurements" Ph.D. dissertation, Air Force Inst of Technology, Wright-Patterson AFB, OH, Mar. 2005 [Online]. Available: http://handle.dtic.mil/100.2/ADA442340

[8] Robust Surface Navigation Program, DARPA Strategic Technology Office [Online]. Available: http://www.darpa.mil/sto/space/rsn.html

[9] M. Rabbat and R. Nowak, "Decentralized source localization and tracking," in *Proc. Int. Conf. Acoustics, Speech, Signal Processing*, Montreal, QC, Canada, May 2004, vol. 3, pp. 921–924.

[10] J. J. Caffery, Jr. and G. L. Stuber, "Overview of radiolocation in CDMA cellular systems," *IEEE Commun. Mag.*, vol. 36, no. 4, pp. 38–45, Apr. 1998.

[11] M. Kieffer and E. Walter, "Centralized and distributed source localization by a network of sensors using guaranteed set estimation," in *Proc. Int. Conf. Acoustics, Speech, Signal Processing*, Toulouse, France, May 2006, vol. 4, pp. 977–980.

[12] L. Cong and W. Zhuang, "Hybrid TDOA/AOA mobile user location for wideband CDMA cellular systems," *IEEE Trans. Wireless Commun.*, vol. 1, no. 3, pp. 439–447, Jul. 2002.

[13] A. Catovic and Z. Sahinoglu, "The Cramér–Rao bounds of hybrid TOA/RSS and TDOA/RSS location estimation schemes," *IEEE Commun. Lett.*, vol. 8, no. 10, pp. 626–628, Oct. 2004.

[14] W. R. Hahn and S. A. Tretter, "Optimum processing for delay-vector estimation in passive signal arrays," *IEEE Trans. Inf. Theory*, vol. 19, no. 9, pp. 608–614, Sep. 1973.

[15] Y. T. Chan and K. C. Ho, "A simple and efficient estimator for hyperbolic location," *IEEE Trans. Signal Process.*, vol. 42, no. 8, pp. 1905–1915, Aug. 1994.

[16] C. H. Knapp and G. C. Carter, "The generalized correlation method for estimation of time delay," *IEEE Trans. Acoust., Speech, Signal Process.*, vol. 24, no. 4, pp. 320–327, Aug. 1976.

[17] C. Mensing, S. Plass, and A. Dammann, "Synchronization algorithms for positioning with OFDM communications signals," in *Proc. 4th Workshop Positioning, Navigation, Communication*, Mar. 2007, pp. 205–210.

[18] T. M. Schmidl and D. C. Cox, "Robust frequency and timing synchronization for OFDM," *IEEE Trans. Commun.*, vol. 45, no. 12, pp. 1613–1621, Dec. 1997.

[19] H. Minn, V. K. Bhargava, and K. B. Letaief, "A robust timing and frequency synchronization for OFDM systems," *IEEE Trans. Wireless Commun.*, vol. 2, no. 4, pp. 822–839, Jul. 2003.

[20] I. F. Progri and W. R. Michalson, "An investigation of a DSSS-OFDM-CDMA-FDMA indoor geolocation system," in *Proc. Position Location Navigation Symp.*, Apr. 2004, pp. 662–670.

[21] P. J. Voltz and D. Hernandez, "Maximum likelihood time of arrival estimation for real-time physical location tracking of 802.11a/g mobile stations in indoor environments," in *Proc. Position Location Navigation Symp.*, Apr. 2004, pp. 585–591.

[22] H. Reddy, M. G. Chandra, P. Balamuralidhar, S. G. Harihara, K. Bhattacharya, and E. Joseph, "An improved time-of-arrival estimation for WLAN-based local positioning," in *Proc. 2nd Int. Conf. Comm. Systems Software Middleware*, Bangalore, India, Jan. 2007.

[23] F. Winkler, E. Fischer, E. Grass, and G. Fischer, "A 60 GHz OFDM indoor localization system based on DTDOA," presented at the 14th IST Mobile & Wireless Comm. Summit, Dresden, Germany, Jun. 2005.

[24] C. Morelli, M. Nicoli, V. Rampa, and U. Spagnolini, "Hidden markov models for radio localization in mixed LOS/NLOS conditions," *IEEE Trans. Signal Process.*, vol. 55, no. 4, pp. 1525–1542, Apr. 2007.

[25] S. H. Yoo, C. Yoo, S. Lee, S. Y. Kim, and S. Yoon, "A novel scheme for positioning error mitigation in OFDM-based on wireless location systems," in *Proc. 9th Intl. Conf. Advanced Comm. Technology*, Feb. 2007, vol. 2, pp. 1267–1270.

[26] O. Bar-Shalom and A. J. Weiss, "Direct position determination of OFDM signals," presented at the IEEE 8th Workshop Signal Processing Advances in Wireless Comm., Helsinki, Finland, Jun. 2007.

[27] A. Urruela and J. Riba, "Efficient mobile location from time measurements with unknown variances in dynamic scenarios," in *Proc. 2004 IEEE 5th Workshop Signal Processing Advances Wireless Comm.*, Jul. 2004, pp. 571–575.

[28] M. Najar and J. Vidal, "Kalman tracking for mobile location in NLOS situations," in *Proc. Personal, Indoor Mobile Radio Comm. (PIMRC)*, 2003, pp. 2203–2207.

[29] N. Patwari, J. N. Ash, S. Kyperountas, A. O. Hero, III, R. L. Moses, and N. S. Correal, "Locating the nodes: cooperative localization in wireless sensor networks," *IEEE Signal Process. Mag.*, vol. 22, no. 4, pp. 54–69, Jul. 2005.

[30] J.-J. van de Beek, M. Sandell, and P. O. Borjesson, "ML estimation of time and frequency offset in OFDM systems," *IEEE Trans. Signal Process.*, vol. 45, no. 7, pp. 1800–1805, Jul. 1997.

[31] J. S. Velotta, "Navigation using orthogonal frequency division multiplexed signals of opportunity" Master's thesis, Air Force Institute of Technology, Wright-Patterson AFB, OH, Sep. 2007 [Online]. Available: http://stinet.dtic.mil/cgi-bin/GetTRDoc?AD=A476762&Location=U2&doc=GetTRDo c.pdf

[32] W. Hoeffding, *A Class of Statistics with Asymptotically Normal Distribution*, S. Kotz and N. L. Johnson, Eds. New York: Springer-Verlag, 1992, vol. I, Breakthroughs in Statistics, pp. 308–334.

Richard K. Martin received dual B.S. degrees (*summa cum laude*) in physics and electrical engineering from the University of Maryland, College Park, in 1999, and the M.S. and Ph.D. degrees in electrical engineering from Cornell University, Ithaca, NY, in 2001 and 2004, respectively.

Since August 2004, he has been an Assistant Professor at the Air Force Institute of Technology (AFIT), Dayton, OH. His research interests include equalization for multicarrier and single-carrier cyclic-prefixed systems; blind, adaptive filters; sparse adaptive filters; navigation and source localization; and cognitive radio. He has authored 16 journal papers, 35 conference papers, and four patents.

Dr. Martin has been elected ECE Instructor of the Quarter three times and HKN Instructor of the Year twice, by the AFIT students.

Jamie S. Velotta received the Master's degree from the Air Force Institute of Technology (AFIT), Dayton, OH in 2007.

He is currently a civilian Electrical Engineer with The Boeing Company, Huntsville, AL, designing wireless architectures for the Department of Homeland Security.

John F. Raquet (M'05) is currently an Associate Professor of electrical engineering at the Air Force Institute of Technology, Wright-Patterson AFB, OH, where he is also the Director of the Advanced Navigation Technology (ANT) Center. He has been working in navigation-related research for over 18 years. His areas of interest include global positioning system (GPS) precise positioning, non-GPS precision navigation, optically aided navigation, navigation using signals of opportunity, integration of MEMS-based inertial measurement units with other sensors, autonomous vehicle navigation and control, and electromagnetic interference and mitigation techniques affecting GPS performance.

Dr. Raquet is a member of the Institute of Navigation (ION).